Characterization of Al-doped ZnO nanorods grown by chemical bath deposition method

Caracterización de nanobarras de Al-doped ZnO crecidos por el método de deposición química en baño

Author:

Sabah M. Ahmed[1]

SCIENTIFIC RESEARCH

How to cite this paper:
Ahmed, Sabah, M., Characterization of Al-doped ZnO nanorods grown by chemical bath deposition method, Duhok, Iraq. Innovaciencia. 2018; 6(1): 1-9.
http://dx.doi.org/10.15649/2346075X.463

Reception date:
Received: 26 April 2018
Accepted: 10 August 2018
Published: 28 December 2018.

Keywords:
ZnO; Al-Doped; CBD; Nanostructure; Nanorods; Structure

ABSTRACT

Introduction: In recent years a metal oxide semiconductors have been paid attention due to their excellent chemical and physical properties. ZnO (Zinc oxide) is considered as one of the most attractive semiconductor materials for implementation in photo-detectors, gas sensors, photonic crystals, light emitting diodes, photodiodes, and solar cells, due to its novel electrical and optoelectronic properties. There are different uses of metal oxide semiconductors such us, UV photodetectors which are useful in space research's, missile warning systems, high flame detectors, air quality spotting, gas sensors, and precisely calculated radiation for the treatment of UV-irradiated skin. ZnO is a metal oxide semiconductors and it is used as a transparent conducting oxide thin film because it has the best higher thermal stability, best resistance against the damage of hydrogen plasma processing and relatively cheaper if one compares it with ITO. **Materials and Methods:** On glass substrates, Al-doped ZnO (AZO) nanorods have been grown by a low -cost chemical bath deposition (CBD) method at low temperature. The seed layer of ZnO was coated on glass substrates. The effect of the Al-doping on the aligned, surface morphology, density, distribution, orientation and structure of ZnO nanorods are investigated. The Al-doping ratios are 0%, 0.2%, 0.8% and 2%. The Aluminum Nitrate Nonahydrate (Al (NO3)3.9H2O) was added to the growth solution, which is used as a source of the aluminum dopant element. The morphology and structure of the Al-doped ZnO nanorods are characterized by field emission scanning electron microscopy (FESEM) and high-resolution X-ray diffractometer (XRD). using the radio RF (Radio frequency) magnetron technique. **Results and Discussion:** The results show that the Al-doping have remarkable effects on the topography parameters such as diameter, distribution, alignment, density and nanostructure shape of the ZnO nanorods. These topography parameters have proportionally effective with increases of the Al-doping ratio. Also, X-ray diffraction results show that the Al-doping ratio has a good playing role on the nanostructure orientation of the ZnO nanorods. **Conclusions:** The Aluminum Nitride Nanohydrate considered as a good Aluminum source for doping ZnONR. It is clear from FESEM results that the Al-doping of ZnONR has a remarkable effect on the surface topography of nanorods for all aluminum doping ratios. From XRD patterns, it concludes that as the Al-doping ratio increases, the reorientation of the nanostructure of ZnO increases towards [100] direction. The results obtained also have shown that the average diameter of a nanorod is increased with increasing the ratio of Al-doping.

[1] Physics Department, Science Collage, University of Duhok, Email: sabma62@uod.ac, Duhok, Iraq.

INTRODUCCTION

In recent years a metal oxide semiconductors have been paid attention due to their excellent chemical and physical properties. ZnO (Zinc oxide) is considered as one of the most attractive semiconductor materials for its implementation in photo-detectors, gas sensors, photonic crystals, light emitting diodes, photodiodes, and solar cells, due to its novel electrical and optoelectronic properties. There are different uses of metal oxide semiconductors such us, UV photodetectors which are useful in space research's, missile warning systems, high flame detectors, air quality spotting, gas sensors, and precisely calculated radiation for the treatment of UV-irradiated skin [1]. ZnO is a metal oxide semiconductors and it is used as a transparent conducting oxide thin film because it has the best higher thermal stability, best resistance against the damage of hydrogen plasma processing and relatively cheaper if one compares it with ITO [2]. However, the resistivity of pure ZnO thin films is high and its conductivity is low. It is usually necessary to promote the conductivity and this can be done by doping ZnO with various dopants and by thermal treatment in a reducing atmosphere [3]. To obtain higher conductivity of ZnO materials, the ZnO has been doped with other dopant materials such as ZnO doped with aluminum AZO, Indium IZO and gallium materials GZO [4-6]. In recent years wide attention has been drawn on inorganic 1D semiconductor nanomaterials (e.g., nanotubes, nanorods, and nanowires) because usually show various significant electronic and photo-electrochemical properties and have a prospective application in photonic and electronic devices [7-11]. ZnO materials have been grown with different techniques, such as chemical vapor deposition (CVD) [12], hydrothermal system process [13], thermal evaporation [14], pulsed laser deposition [15], sputtering [16], and etc.

In this paper, a convenient low cost, and low growth temperature chemical bath deposition (CBD) method was used to synthesis pure ZnO nanorod and aluminum doped ZnO nanorods with different doping concentration. Also, the effect of Al-doped ZnO on the morphology and structure of ZnO nanorods have been investigated.

MATERIALS AND METHOD

All chemicals are provided from Sigma Aldrich Company which they are of analytical grade and have been used as starting materials without any further purification. In this research, the ZnO coated glass (seed layer) has been used as a base for growing ZnO nanorods (ZnO NR). There are two steps needed to complete this process. The first step is the cleaning of the substrate in an ultrasonic cleaner using ethanol, acetone and deionized water for 20 min respectively and then dehydrated by nitrogen gas. The second step is, an RF magnetron sputter coater is employed using high purity ZnO target (99.999% purity) [17]. ZnO seed layers of 150 nm thick are deposited on the glass substrates under argon gas at a pressure about 5 *10-3 Torr and the power of RF sputtering is 150 Watt for 20 min. The coated ZnO seed layer on the glass substrates is annealed under atmosphere using tubular furnace at about 360 oC for 2 h and this step is very important to enhance the structural and optical properties of the ZnO seed layer. The Al-doped ZnO nanorods (AZO) are grown on the seed layer using a low-temperature CBD method.

The precursor's materials are Hexamethylenetetramine ($C_6H_{12}N_4$), Zinc Nitrate Hexahydrate (Zn

$(NO_3)_2.6H_2O$) and deionized water. The equal molar concentration of (Zn $(NO_3)_2.6H_2O$) and HMTA ($C_6H_{12}N_4$) are separately dissolved in deionized water at 80 oC and a magnetic stirrer is used to mix them together. Various precursor concentrations (0%, 0.2%, 0.8%, and 2%) of Aluminum Nitrate Nonahydrate (Al $(NO_3)_3.9H_2O$) are used to assay the influence of Al-doping ratio on the growth process, structure, and morphology of ZnO NR. The infectious ZnO seed layers were inserted vertically in the CBD reactor. To study the influence of the Al-doping on the surface topography and structure of ZnO NR, the CBD reactor is set inside an oven at 95 ºC for 5 hrs. After the growth process of ZnO NR is completed, the substrates have been taken out from the CBD reactor and washed with deionized water to clean it's from the remaining salts, and then dehydrated by nitrogen gas.

The Al-doped ZnO and undoped nanorods are tested using field-emission scanning electron microscope (FESEM: FEI Nova nano SEM 450, Netherlands and Leo-Supra 50 VP, Carl Zeiss, Germany) and high-resolution XRD (HR-XRD) system X-Pert Pro MRD model with CuKα (λ = 0.154050 nm), 2θ scanning range was between 20° and 80° to study the surface morphology and structure respectively.

RESULTS

The surface morphology of the undoped (ZNs) and Al-doped ZnO (AZO) nanorods grown on glass substrate by chemical bath deposition method at 95 ºC for 5 h are shown in figure 1. Figure (1a) shows the morphology of undoped ZnO nanorods while figures (1b), (1c), and (1d) are shown the morphology of doped ZnO nanorods in different doping percentages.

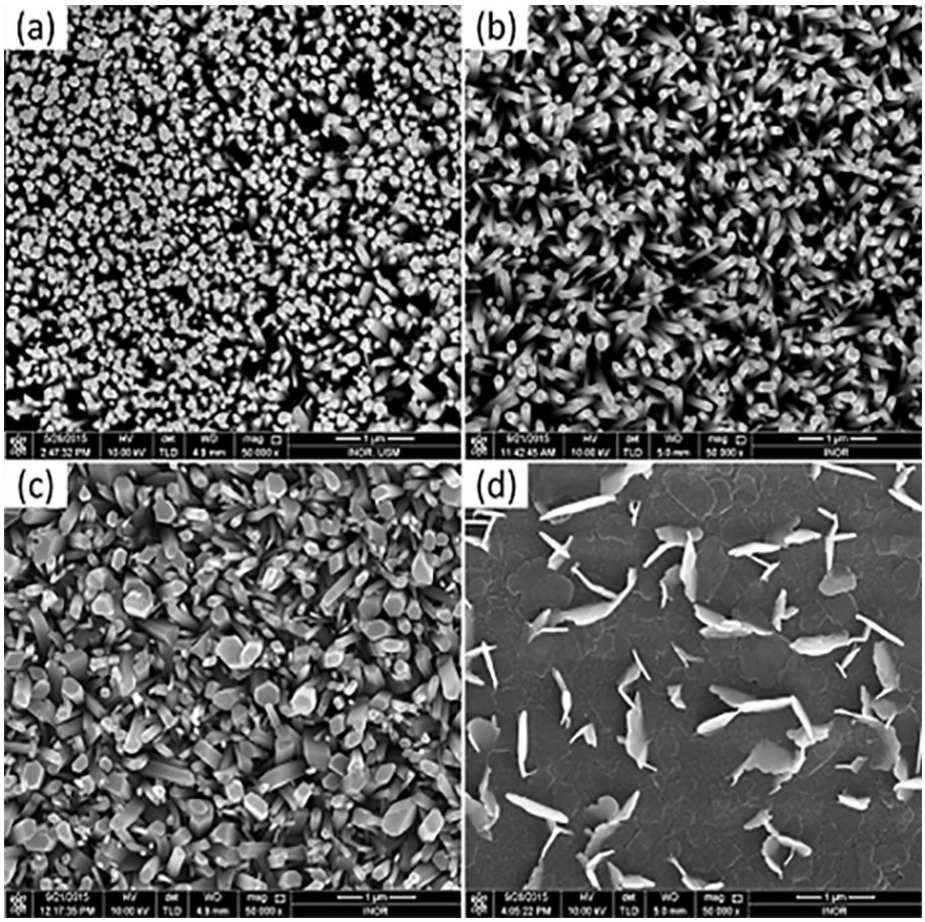

Figure 1. FESEM Image of Undoped and Al-doped ZnO nanorods fabricated by CBD method

The X-ray diffraction (XRD) patterns of pure ZnO nanorods and Al-doped ZnO nanorods grown on glass substrates are displayed in figure 2. The crystal structure of the undoped (pure) ZnO nanorods prepared by CBD is shown in figure (2a). Also figure 2 shows the crystal structure of the doped ZnO nanorods in different doping percentages as in (2b), (2c), and (2D).

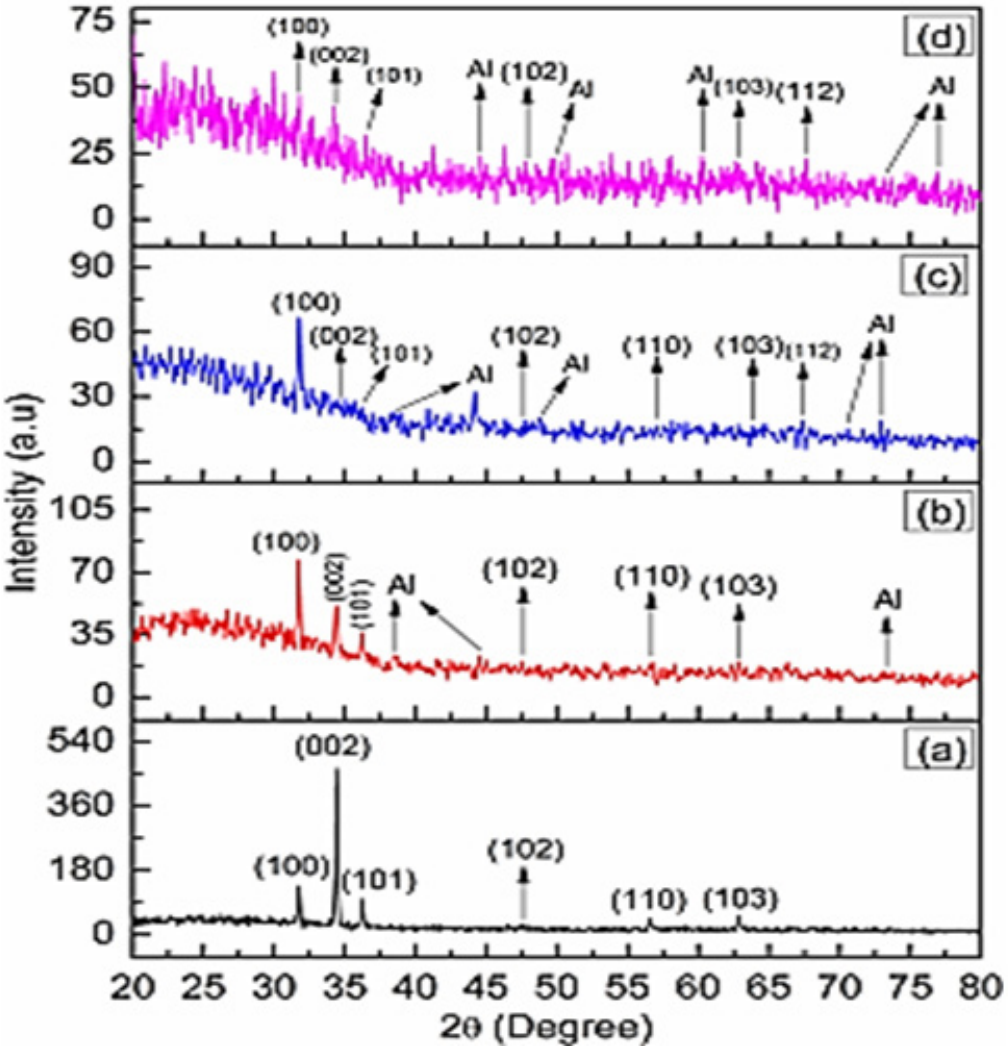

Figure 2. X-Ray diffraction patterns of ZnO nanorods (a) 0% Al, (b) 0.2% Al, (c) 0.8% Al and (d) 2% Al

The lattice parameters and the interplanar distance of wurtzite hexagonal structure of ZnO nanorods are summarized in tables 1, 2 and 3 and calculated according to Bragg's law [18].

$$2d\sin\theta = n\lambda \quad (1)$$

Where d is the interplanar distance, n is the order of diffraction that usually is 1, λ is X-ray wavelength. The lattice constants a and c of the ZnO wurtzite hexagonal structure can be found using Bragg's law, as it's shown in tables 1,2 and 3 [19, 20].

$$a = \sqrt{\frac{1}{3}}\frac{\lambda}{\sin\theta} \quad (2)$$

$$c = \frac{\lambda}{\sin\theta} \quad (3)$$

Where θ is the angle of the diffraction peak.

The strain (Ɛc) and perpendicular strain (Ɛa) of the ZnO nanorod grown on the glass substrate along c-axis and a- axis respectively can be obtained by using the following equation, and are described in the tables 1, 2 & 3. (Ɛc) and (Ɛa) are calculated according to the following equations [21, 22]:

$$\varepsilon_c = \frac{c - c_o}{c_o} * 100\% \quad (4)$$

$$\varepsilon_a = \frac{a - a_o}{a_o} * 100\% \quad (5)$$

Where co and ao are represents the standard lattice constant for unstrained ZnO which are equal to 5.2151 Å & 3.2535 Å, respectively. A positive value of strain is related to the tensile strain and indicates an expansion in lattice constant, whereas a negative value is related to the compressive strain and indicates a lattice contraction.

The Average particle size of ZnO nanorods fabricated by CBD method is calculated using the Debye Scherer formula. [23]:

$$D = \frac{K\lambda}{\beta \cos\theta} \quad (6)$$

Where k is a constant which is taken to be 0.9, λ is the wavelength of the X-ray (0.154056 nm), β is the full width at half maximum of the peak and the θ is the Braggs diffraction angle. The structural properties of the ZnO nanorods are shown in Table 1, 2 and 3. The dislocation density (δ), which represents the amount of defects in the crystal, is estimated from the following equation [18]:

$$\delta = \frac{1}{D^2} \quad (7)$$

Where D is the average particle size of the ZnO nanorods

Table 1. lattice parameters and Structure properties of the ZnO nanorods of (002) plane

Sample	Plane	FWHM	2θ	a (Å)	c (Å)	ε_c	ε_a	d (Å)	D (nm)	δ (nm^{-2})
0.0% AZO	002	0.7872	34.3750	3.01004	5.21354	-0.02986	-7.483	2.6068	10.5636	0.0090
0.2% AZO	002	0.4576	34.3733	3.01018	5.21379	-0.02506	-7.479	2.6069	18.1718	0.0030
0.8% AZO	002	0.3201	34.325	3.01429	5.22091	0.11137	-7.352	2.6105	25.9772	0.0015
2.0% AZO	002	0.1111	34.275	3.01856	5.22830	0.25302	-7.221	2.6141	75.0104	0.0002

Table 2. lattice parameters and Structure properties of the ZnO nanorods of (100) plane

Sample	Plane	FWHM	2θ	a (Å)	c (Å)	Σ_c	Σ_a	d (Å)	D (nm)	δ (nm^{-2})
0.0% AZO	100	0.2479	31.775	3.2492	5.62778	7.91308	-0.132	2.8139	33.3197	0.00090
0.2% AZO	100	0.3640	31.775	3.2492	5.62778	7.91308	-0.132	2.8139	22.6918	0.00194
0.8% AZO	100	0.4154	31.792	3.2475	5.62476	7.85521	-0.186	2.8124	19.8848	0.00253
2.0% AZO	100	0.5904	31.825	3.2442	5.61916	7.74791	-0.285	2.8096	13.9919	0.00511

Table 3. lattice parameters and Structure properties of the ZnO nanorods of (101) plane

Sample	Plane	FWHM	2θ	a (Å)	c (Å)	Σ_c	Σ_a	d (Å)	D (nm)	δ (nm^{-2})
0.0% AZO	101	0.2254	36.225	2.8610	4.95555	- 4.97691	- 12.06	2.4778	37.0710	0.00073
0.2% AZO	101	0.3257	36.175	2.8649	4.96217	- 4.84997	- 11.94	2.4810	25.6594	0.00152
0.8% AZO	101	0.3006	36.007	2.8779	4.98460	- 4.41980	- 11.55	2.4923	27.7887	0.00129
2.0% AZO	101	0.0999	36.475	2.8421	4.92273	- 5.92273	- 12.64	2.4613	83.6529	0.00014

DISCUSSION

Figure (1a) shows the undoped (pure) ZnO, it can be clearly seen that the ZnO NR has a uniform distribution and density with tiny gaps in between, uniform orientation and vertically well-aligned growth with average diameters of 83nm. The 0.2% Al-doped ZnO nanorods (0.2% AZO) is shown in figure (1b), one can observe that the AZO nanorod has good distribution, different orientations and vertically aligned with the average diameter of 103 nm. It can be concluding from figures 1a and 1b that the AZO has less compaction morphology and not vertically well aligned as compared to those of undoped ZnO NR. Figure (1c) shows the 0.8% Al-doped ZnO nanorods (0.8% AZO) grown on a glass substrate. It is noted that the AZO nanorods have also different orientations, different lengths, not vertically well aligned and have good distribution with an average diameter of 259 nm. In addition, the 2% Al-doped ZnO nanorods fabricated on the ZnO seed layer-coated glass substrate at 95 ºC is shown in figure 1(d). It can be seen that the AZO nanorods like nanosheets over the very dense nanorods with nanosheets lengths of about 699 nm and diameters of about 280 nm and the average diameters of nanorods are 658.6 nm. The results of the average diameters are in good agreement with the reported values in the

literature [24, 25]. The crystal structure of the undoped (pure) ZnO nanorods prepared by CBD is shown in figure (2a). It can be notice that ZnO nanorods have hexagonal structure, remarkably sharp peak at 2θ=34.3750, which is assigned to be the (002) peak of hexagonal structure and with (FWHM) is 0.7872, and this is meaning that the most ZnO nanorods are grown along c-axis [26]. Figure (2b) shows the XRD pattern of the 0.2% Al-doped ZnO nanorods, from the figure one can found that the prominent sharp peak at 2θ=31.775, which is assigned to be the (100) peak with (FWHM) is 0.3640, and the other peaks belong of ZnO are appeared. That means that the most of Al-ZnO nanorods are grown along (100) direction, the diffraction peaks of Al are appeared which is confirmed the Al doping of ZnO nanorods. Also figure (2c) shows the XRD pattern of 0.8% of Al-doped ZnO nanorods on glass substrate. It is observed that the sharp peak is appeared at 2θ=31.792 with (FWHM) equal to 0.4154 with weakness peaks of ZnO than the peaks of ZNR and notable peaks of Al, it means that all AZO nanorods are growth along (100) plane. In addition, the crystal structure of 2% Al-doped ZnO nanorods fabricated by CBD method is shown in figure (2d). It can clearly see that the XRD pattern is very noisy not remarkable sharp peak of ZnO nanorods, that means that film destroyed with high ratio of Al doped in ZnO nanorod and this confirm with FESEM image, but the peaks of ZnO and Al are appeared [27]. The lattice parameters have been listed in tables 1, 2, and 3 and are found to be in good agreement with the reported standard values (JCPDS cards No. 01-080-0074). The particle size are increases with increase the ratio of doping Al in ZnO nanorods along (002) plan as shown in table 1, but along (100) plane the particle size are decreases with increase the ratio of the Al doped ZnO nanorods as displayed in table 2 and the particle size along (101) plane of pure ZnO nanorods is about 37.07 nm is decreases to 25.6594 nm when increase the ratio of doping Al to 0.2% in the ZnO nanorods, but with increasing the ratio of doing Al to 0.8% and 2% in the ZnO nanorods the particle size started to increase as shown in the table 3

CONCLUSIONS

The Aluminum Nitride Nanohydrate considered as a good Aluminum source for doping ZnO NR. It is clear from FESEM results that the Al-doping of ZnO NR has a remarkable effect on the surface topography of nanorods for all aluminum doping ratios. From XRD patterns, it concludes that as the Al-doping ratio increases, the reorientation of the nanostructure of ZnO increases towards [100] direction. The results obtained also have shown that the average diameter of a nanorod is increased with increasing the ratio of Al-doping.

REFERENCES

1. Saxena K, Kumar A, Malik N, Kumar P, and Jain V K, et al. Ultraviolet sensing properties of polyvinyl alcohol-coated aluminium-doped zinc oxide nanorods, Bull. Mater. Sci., 2014 April; 37(2): 295–300. https://doi.org/10.1007/s12034-014-0653-6
2. T.K, B. H and Aiura Y, et al. photovoltaic effect observed in transparent p-n heterojunctions based on oxide semiconductors, Thin Solid Films, 2003; 445: 327-331. https://doi.org/10.1016/S0040-6090(03)01177-5
3. Hsu C. and Chen D, et al. Synthesis and conductivity enhancement of Al-doped ZnO nanorod array thin films, Nanotechnology. 2010; 21(28): 285603. https://doi.org/10.1088/0957-4484/21/28/285603
4. Raimondi D. L, et al.. High resistivity transparent ZnO thin films, J. Vaccum Science Technol., 1969; 7: 96-99. https://doi.org/10.1116/1.1315841

5. Oda J, et al. Improvements of spatial resistivity distribution in transparent conducting Al-doped ZnO thin films deposited by DC magnetron sputtering. Thin Solid Films, 2010; 518: 2984-2987. https://doi.org/10.1016/j.tsf.2009.09.174
6. Yen W., et al. Influences on optoelectronic properties of damp heat stability of AZO and GZO for thin film solar cells. Advanced Materials Research: Multi-Functional Materials and Structures II, 2009; 79: 923-926. https://doi.org/10.4028/www.scientific.net/AMR.79-82.923
7. Law M, Greene L E, Johnson J C, S. R and Yang P D, et al. Nanowire dye-sensitized solar cells. Nature Mater, 2005; 4: 455. https://doi.org/10.1038/nmat1387
8. Zhen G, Dongxu Z, Yichun L, Dezhen S, Jiying Z, Binghui Li, et al. Visible and ultraviolet light alternative photodetector based on ZnO nanowire/n-Si heterojunction. Applied. Physics. Lett. 2008; 93: 163501. https://doi.org/10.1063/1.3003877
9. Vayssieres L. Growth of Arrayed Nanorods and Nanowires of ZnO from Aqueous Solutions. Advance Mater, 2003; 15: 464. https://doi.org/10.1002/adma.200390108
10. Greene L. Law M, Goldberger J, Kim F, Johnson J, Zhang Y, Saykally R , Yang P,et al. Angew. Chem., Int. Edn, 2003; 42: 3031. https://doi.org/10.1002/anie.200351461
11. Sun Y, Riley J, Michael N, et al. Mechanism of ZnO Nanotube Growth by Hydrothermal Methods on ZnO Film-Coated Si Substrates. Journal Physics. Chem. B, 2006; 110: 15186. https://doi.org/10.1021/jp062299z
12. Natsume Y, Sakata H, et al. Mater. Chem. Phys.,2002; 78: 170. https://doi.org/10.1016/S0254-0584(02)00314-0
13. Juarez S., Silver T, A Oritz, E Zironi, Rickards J,et al. Electrical and optical properties of fluorine-doped ZnO thin films prepared by spray pyrolysis. Thin Solid Films, 1998; 333: 196. https://doi.org/10.1016/S0040-6090(98)00851-7
14. Yamamoto Y, Saito K, Takakashi K, Konagai M, et al. Sol. Energy Mater. Sol. Cells. 2001; 65: 125. https://doi.org/10.1016/S0927-0248(00)00086-6
15. Tang W and Cameron D C, Aluminum-doped zinc oxide transparent conductors deposited by the sol-gel process, Thin Solid Films, vol. 238, pp. 83, 1994. https://doi.org/10.1016/0040-6090(94)90653-X
16. Herrero J and Guillen C, et al. Improved ITO Thin Films for Photovoltaic Applications With a Thin ZnO Layer by Sputtering. Thin Solid Films, 2004; 451/452: 630. https://doi.org/10.1016/j.tsf.2003.11.050
17. Abdulrahman A, Ahmed S, Ahmed N, Almessiere M, et al. Different Substrates Effects On The To raphy and the structure Of The ZnO NR Grown By Chemical Bath Deposition Method. Digest Journal of Nanomaterials and Biostructures, 2016; 11 (3): 1007 – 1016.
18. Abdulrahman A, Ahmed S, Ahmed N, and Almessiere, et al. Novel Process Using Oxygen And Air Bubbling In Chemical Bath Deposition Method For Vertically Well Aligned Arrays Of Zno Nanorods. Digest Journal of Nanomaterials and Biostructures, 2016; 11(4): 1073-1082.
19. Kashif M. Hashim U, Ali M, Syed M, Rusop M, Ibupoto Z, Willander M, et al. Effect of Different Seed Solutions on the Morphology and Electro optical Properties of ZnO Nanorods. Hindawi Publishing Corporation Journal of Nanomaterials, 2012; 2012: Article ID 452407, 6 pages. https://doi.org/10.1155/2012/452407
20. Suryanarayana C, Norton G, et al. X-Ray Diffraction: A Practical Approach. Springer Science and Business Media, 1998; LLC, 233 Spring Street, New York, NY 10013, USA: Plenum Press.
21. Warren B. X-ray Diffractio Courier Dover Publications, New York, 1969.
22. Tsay C, Fan K, Chen S, Tsai C, et al. Preparation and characterization of ZnO transparent semiconductor thin films by sol–gel method. Journals of Alloys and Compounds, 2010; 495(1): 126-130. https://doi.org/10.1016/j.jallcom.2010.01.100
23. Cullity B. Elements of X-ray Diffraction second edition, Addison Wesley, 2007.
24. Hsu C, Chen D, et al. Synthesis and conductivity enhancement of Al-doped ZnO NR array thin films. Nanotechnology, 2010; 21: 285603. https://doi.org/10.1088/0957-4484/21/28/285603

25. Wang L, Lin B, Hung M, Zhou L, Panin G, Kang T, Fu D,et al. Optical and electrical properties of hydrothermally grown Al-doped ZnO nanorods on graphene/Ni/Si substrate. Solid-State Electronics, 2013; 82: 99–102. https://doi.org/10.1016/j.sse.2013.01.012
26. Abdulrahman A, Ahmed S, Ahmed N, et al. The Influence of The Growth Time on the Size and Alignment of ZnO Nanorods. Science Journal of University of Zakho, 2017; 5(1): 128-135. https://doi.org/10.25271/2017.5.1.313
27. Yang-Ming L, Jian-Fu T, et al. Electro-optical and structural properties of Al-doped ZnO nanorod arrays prepared by hydrothermal process. International Journal of Science and Engineering, 2013; 3(2): 11-15.